applied sciences

MDPI

Article

An Experimental Study on the Seismic Performance of a Replaceable Steel Link System Acting as a Structural Fuse

Kyong Min Ro , Min Sook Kim and Young Hak Lee *

Department of Architectural Engineering, Kyung Hee University, Deogyeong-Daero 1732, Yongin 17104, Republic of Korea; kyongmin@khu.ac.kr (K.M.R.); kimminsook@khu.ac.kr (M.S.K.)
* Correspondence: leeyh@khu.ac.kr; Tel.: +82-31-201-3815

Abstract: This study investigated the seismic performance of reinforced concrete columns retrofitted with Replaceable Steel Links (RSLs), focusing on the effects of varying sliding slot lengths and torsional loads. The RSL system, known for its simple construction and effective seismic performance, was analyzed to assess the feasibility of substituting damaged steel links post-earthquake, using the system as a structural fuse. The experimental results highlighted the role of sliding slot lengths in delaying the initiation of shear cracks, especially under eccentric lateral loads. The RSL system exhibited notable torsional resistance, showing only a 10% decrease in maximum load capacity, even with a two-fold increase in the eccentric distance. Furthermore, with an increase in sliding slot length, the difference in cumulative energy dissipation attributable to augmented eccentric distances reached approximately 50%, indicating a notable impact of sliding slot length on the system's ability to resist torsion. Consequently, it is recommended that the length of the sliding slot be based on the specific seismic design objectives when employing the RSL system as a structural fuse. The post-experiment inspection revealed no deformation in the steel plates, and the buckled steel links could be effortlessly replaced by loosening the high-tensile bolts in the slots. These findings demonstrate the RSL system's efficiency as a structural fuse.

Keywords: seismic retrofitting; brace; structural fuse; replaceable steel link

Citation: Ro, K.M.; Kim, M.S.; Lee, Y.H. An Experimental Study on the Seismic Performance of a Replaceable Steel Link System Acting as a Structural Fuse. *Appl. Sci.* **2024**, *14*, 2358. https://doi.org/10.3390/app14062358

Academic Editors: Wen-Hsiang Hsieh, Jia-Shing Sheu and Minvydas Ragulskis

Received: 31 January 2024
Revised: 27 February 2024
Accepted: 8 March 2024
Published: 11 March 2024

1. Introduction

Recent studies on the seismic retrofitting of reinforced concrete columns have placed a notable emphasis on the utilization of high-performance materials, including high-strength concrete and fiber-reinforced polymers (FRPs). Furthermore, there is a growing focus on the development of effective techniques for retrofitting existing structures. The introduction of advanced techniques, including rapid and cost-effective repairs of earthquake-damaged buildings, as well as numerical modeling and simulation techniques for more accurate assessment of a building's seismic performance, is also a trend in current research [1–5]. Attari et al. [1] conducted experimental research on reinforcing concrete structures using FRPs. Attari et al. [1] investigated the deformability of the specimens after reinforcement, with a view to enhancing the seismic performance of reinforced concrete beam–column joints. Yao et al. [2] studied the seismic performance of corroded RC columns reinforced by textile-reinforced concrete. Nasab et al. [3] proposed a seismic reinforcement method using viscoelastic dampers to prevent shear deformation. Cheng et al. [4] fabricated a 1/5 scale model of an RC frame reinforced with RC infill walls with mega-braces (RCIWMB) and evaluated its seismic performance through shaking table tests. They compared the seismic performance by producing specimens with RCIWMB arranged vertically and intersected. Ferraioli et al. [5] proposed a design method for the seismic retrofit of reinforced concrete buildings using aluminum multi-stiffened shear panels as dampers, and its effectiveness has been validated using nonlinear response-history analysis. Seismic design has allowed inelastic deformation in structures, using hysteretic behavior to dissipate seismic energy.

However, this leads to damage and permanent deformations in structures, resulting in high repair costs. As an alternative, recent seismic designs have implemented the use of structural fuses [5]. In the seismic design and the retrofitting of structures, considering structural fuses means sacrificing these members to disperse seismic energy while maintaining the performance of the structural elements. Structural fuses enter the inelastic region before other structural members, absorbing seismic energy and concentrating damage during earthquakes. After an earthquake, only these fuse elements need replacement, making repairs easier and more cost-effective. In the seismic retrofitting of reinforced concrete structures, structural fuses often use metallic materials for dampers or buckling-restrained braces (BRBs), with the main advantage being their quick repair.

Consequently, research on the seismic retrofitting of reinforced concrete structures is focused on evaluating the dynamic behavior of structures with retrofitting members to assess whether they can function as structural fuses [6–10]. Structures with structural fuses involve complex parameters, requiring nonlinear time history analysis in the design. Therefore, studies on the analysis techniques of structural fuses are also prevalent. Vargas and Bruneau [6] presented a simple and reliable design procedure for structures using BRBs as structural fuses. EI-Bahey et al. [7] applied BRBs, commonly used as structural fuses, to a 2/3-scale model and conducted quasi-static tests to observe their effect on the seismic performance of a complete bridge. The experiments confirmed that adding structural fuses increased the system's strength and stiffness and effectively dissipated seismic energy. Nikoukalam and Dolatshahi [8] noted that, in moment-resisting frames (MRF), the beam span-depth ratio should be designed to allow sufficient length of plastic hinges at the beam ends. They highlighted the issue of over-designing the structure and foundation in the current design procedures for steel MRFs. To overcome this issue, they introduced a new shear structural fuse for MRFs. The shear structural fuse, designed as a sacrificial member to dissipate seismic energy through shear deformation, weakens the shear strength in the middle of the beam. Irvani et al. [9] confirmed the dynamic behavior of a Simpson Strong-Tie (SST) connection using a low-yield-point (LYP) T-stub fuse, which protects structural members at the beam–column joint. The finite element analysis was performed on 15 models with SST connections, confirming that they serve as structural fuses. Farzampour [10] grouped commonly used structural steel fuses into three types based on their characteristics and analyzed their seismic performance in actual buildings through finite element analysis. The structural fuses were categorized into group 1: a single row of links (e.g., eccentrically braced system (EBF), linking beam and linked column applications), group 2: multiple rows of links with multiple rows of dampers (e.g., bay bridge application), and group 3: perimeter rows of links (e.g., steel shear walls). Ghadami et al. [11] and Zhuang et al. [12] proposed a seismic retrofitting method using a steel link. The seismic retrofitting method employing a steel link has been confirmed to effectively enhance both stiffness and strength under cyclic loading. The analysis revealed that structural fuses can improve the energy dissipation capability but also highlighted issues including replaceability, cost, and complex design requirements. Recent trends have involved proposing and evaluating seismic retrofit materials that can function as structural fuses with easy replacement details [13–17]. In particular, the seismic retrofitting method using a steel link can be considered to function as a structural fuse, given the replaceability of the steel link. However, studies proposing the seismic retrofitting method with a steel link, such as [11,12], involve coupling the steel link to a moment frame and combining it with a brace system. This configuration requires a considerable amount of installation space.

The previous study [18] introduced the concept of the Replaceable Steel Link (RSL) system and validated its seismic performance through experiments. This current study focuses on a distinct aspect of RSL utilization that was not addressed previously. While the initial conceptualization of the RSL system involved its connection to structures via bolts as a steel fuse, the feasibility of the RSL system specifically as a structural fuse remained unconfirmed in the previous study [18]. A unique aspect of this study is the examination of whether RSL, when using seismic retrofitting solutions, allows for the replacement of deformed steel links after seismic events. This entails subjecting columns to experiments with varying eccentricities, a crucial parameter influencing torsional effects. The main goal of this study is to evaluate not only the seismic performance of RSL but also the practicality and efficacy of replacing deformed steel links after seismic events. In essence, this study distinguishes itself from the previous study [18] by shifting the focus from the seismic retrofitting effectiveness of RSL in a general structural aspect to its applicability as a replaceable structural fuse under torsional loads. This perspective contributes to a comprehensive understanding of the versatility and adaptability of the RSL system in seismic design.

2. Concept of the Replaceable Steel Link (RSL)

The RSL method, as illustrated in Figure 1, involves installing steel links at the ends of columns to resist seismic forces. This differs from conventional bracing methods, which are typically installed diagonally across beam–column frames. The RSL method comprises a steel link designed to resist lateral loads through compression and a steel plate that connects it to existing structural members, as shown in Figure 2. The steel plate is anchored to the structural member using chemical anchors. Designed for ease of installation and replacement, the steel link is lightweight and tubular, connected to the steel plate via a welded hinge and bolt. The hinge on the bottom plate, which attaches to the horizontal member, is designed with a sliding slot. This characteristic enables the steel link to move laterally, accommodating the lateral displacement of the reinforced concrete column. The RSL method is engineered to act as a structural fuse within the building, dispersing seismic energy during an earthquake and ensuring occupant safety.

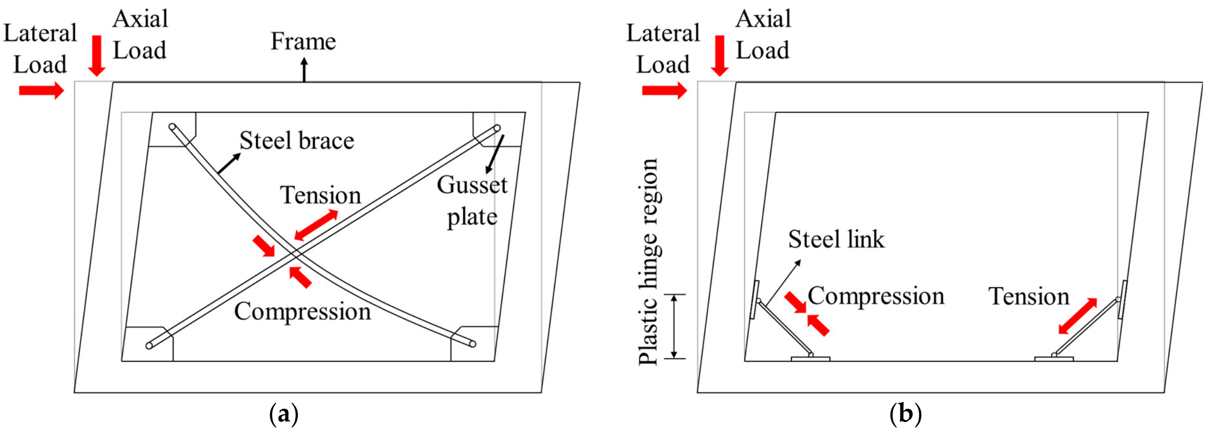

Figure 1. Comparison of the RSL system and conventional brace system: (**a**) brace and (**b**) RSL.

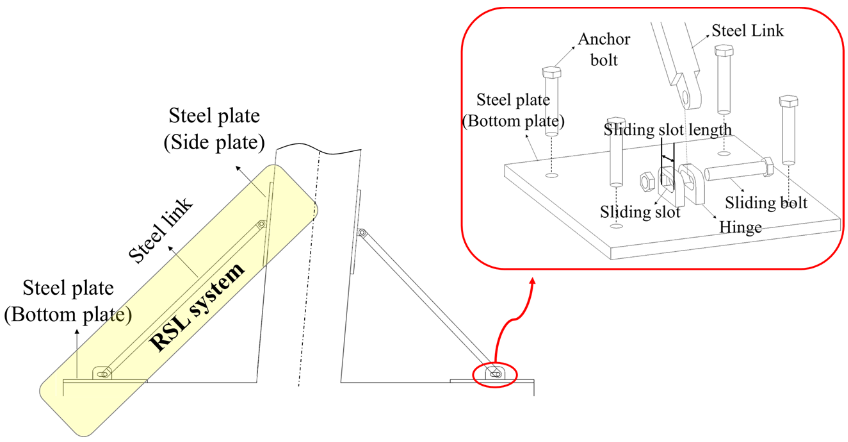

Figure 2. Components of the RSL system.

The construction process of the RSL method involves the preparation of the surface of the existing element followed by the adjustment of the steel plate and the connection of the steel link to the plate through a sliding bolt attached to a welded hinge. Unlike conventional bracing methods applied to beam–column frames, the RSL method can enhance the overall seismic performance of a structure when applied to a single column, which is especially beneficial in structures with limited retrofitting space or where open spaces like pilotis are required. Additionally, the ease of replacing the steel link after damage is a significant advantage of the RSL method. The steel link is joined to the existing structural member through the steel plate and anchor bolts, facilitating straightforward replacement if damaged.

Figure 3 illustrates the behavior characteristics of the RSL system, showcasing two distinct stages contingent upon the sliding slot's length.

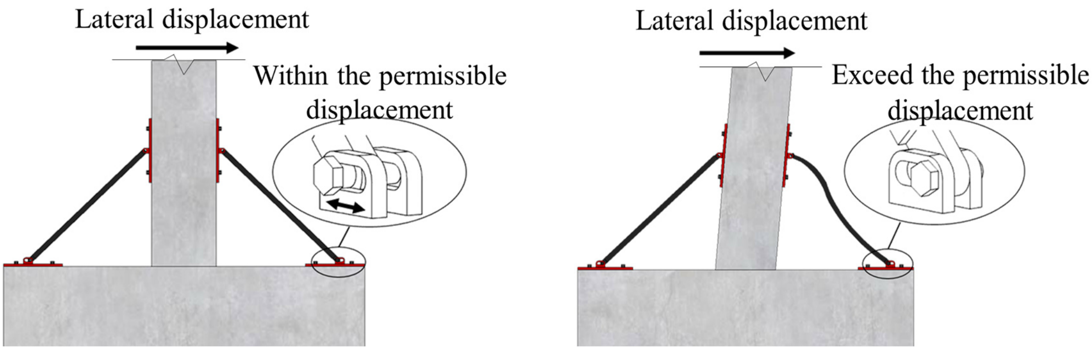

(**a**) (**b**)

Figure 3. Behavior of the RSL system: (**a**) stage 1 and (**b**) stage 2.

(1) stage 1: In cases where the lateral displacement of the column falls within the sliding slot's length, remaining within the allowable range of displacement.
(2) stage 2: When the lateral displacement of the column surpasses the acceptable range.

Under moderate wind or seismic conditions, the lateral displacement remains confined within the acceptable range. During this stage, the column primarily sustains the load through the frictional force generated between the sliding slot and bolt, along with the confinement offered by the RSL system. As the lateral load magnitude escalates, the steel link engages with the end of the sliding slot, resisting the lateral load akin to conventional bracing methods. The adjustability of the sliding slot's length facilitates the tuning of seismic energy dissipation by the RSL system, underscoring its role as a structural fuse. Furthermore, the RSL system is devised to enhance the seismic performance of the entire column, even when exclusively installed in the plastic hinge zones where damage concentrates in reinforced concrete columns. This design allows for the straightforward replacement of damaged steel links without the need for heavy machinery.

3. Experimental Program

3.1. Specimen Details

In this study, the seismic performance of reinforced concrete columns retrofitted with RSL was evaluated to assess the role of RSL as a structural fuse. The cyclic loading tests were conducted on five test specimens of reinforced concrete columns retrofitted with RSL. To investigate the behavior of the RSL-retrofitted specimens in both stage 1 and stage 2, the length of the sliding slot was varied. Additionally, to examine the behavior of retrofitted specimens under a torsional load, which occurs during real earthquakes, the magnitude of the torsion was altered by changing the eccentric distance of the lateral force applied to the specimens. The eccentricity distance refers to the distance offset from the centerline of the column. Considering the experimental conditions designed to induce maximum bending and torsion in the column, the eccentric distance was determined to be larger than the core section of the column, measuring 62.5 mm [19,20]. Therefore, the eccentric distance was set at 65 mm. Additionally, to investigate the influence of torsion, an eccentric distance of 130 mm, twice the value of 65 mm, was also adopted. The experimental variables are listed in Table 1. A previous study [18] examined the seismic performance of RSL compared to non-retrofitted concrete columns. This study specifically concentrates on evaluating the torsional behavior of RSL-retrofitted specimens, an aspect that has already been validated in previous studies and assessing the replaceability of the steel link after a seismic event. Therefore, it is important to note that non-retrofitted concrete column specimens were not used as a control specimen in this study. The determination of the sliding slot length was grounded in the initiation points of flexural and shear cracks in reinforced concrete columns, as identified in previous research [18] through cyclic loading testing. In conceptual terms, a sliding slot length of 5 mm indicates that the steel link begins to resist loads following the occurrence of flexural cracks in the reinforced concrete column. On the other hand, a sliding slot length of 10 mm implies that resistance initiation takes place after the development of shear cracks. Figure 4 is intended to introduce the notation of specimens.

Table 1. Details of the specimens.

No.	Specimen	Retrofitting Method	Eccentric Distance (mm)	Sliding Slot Length (mm)	Point at Which the Steel Link Begins to Resist Load
1	NE-10	RSL	0	10	Shear crack initiation
2	E130-10		130		
3	NE-5		0	5	Flexural crack initiation
4	E65-5		65		
5	E130-5		130		

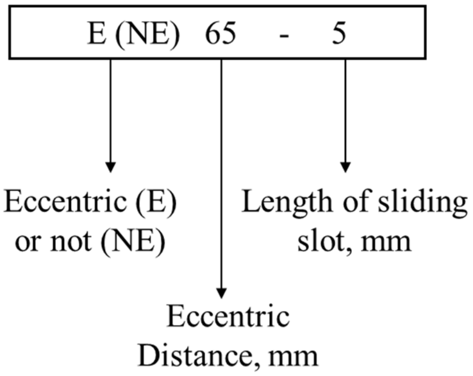

Figure 4. Notation of specimens.

The test specimens consisted of a reinforced concrete column, a foundation, and the RSL. The column had a square cross-section, with each side measuring 250 mm and a height of 2050 mm. The top 250 mm of the column was allocated for the application of lateral forces. The foundation, designed for the installation of the RSL and to secure the specimen, measured 1400 mm in width, 425 mm in height, and 1270 mm in length. All specimens were designed following the guidelines of ACI 318-19 [21], ensuring that the design was consistent with the non-seismic detailing of reinforced concrete columns. The longitudinal reinforcement was four deformed bars with a diameter of 22 mm and a yield strength of 400 MPa. Stirrups were made of deformed bars with a diameter of 10 mm and a yield strength of 400 MPa, spaced at 125 mm, which is half the minimum column dimension of 250 mm. The columns were cast using concrete with a compressive strength of 24 MPa, while the foundation was made of concrete with a compressive strength of 30 MPa to prevent premature failure. The material properties of the specimens were determined through experimentation, and the average values of three specimens were considered. The experimental results are presented in Figure 5. The 28-day compressive strength of the concrete used in fabricating the column was found to be 24.3 MPa, while for the foundation, it was 30.8 MPa. The yield strengths of the steel plate and reinforcing bar, determined through experimentation, were 275.4 MPa and 401 MPa, respectively.

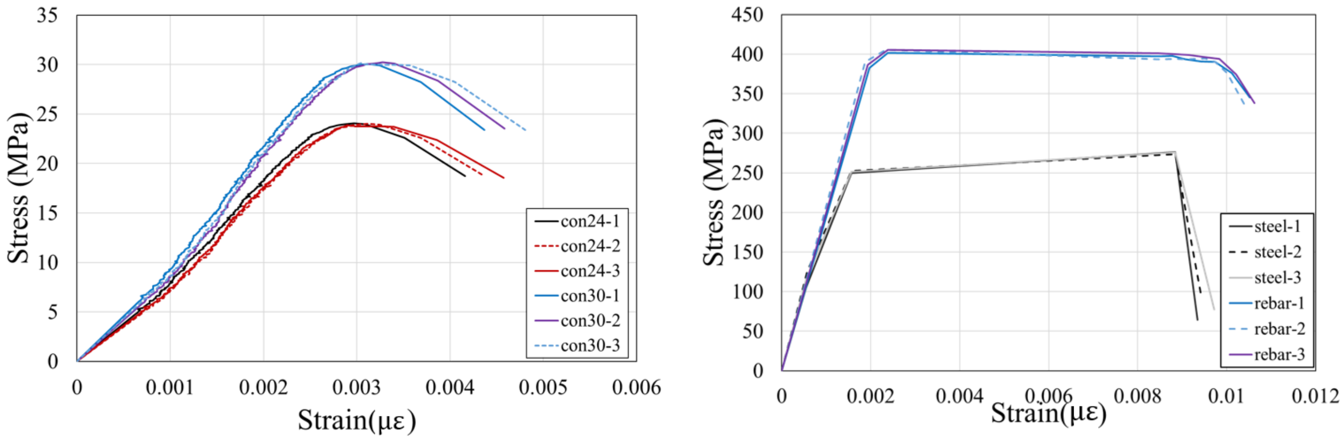

(**a**) (**b**)

Figure 5. Material properties: (**a**) concrete and (**b**) steel and rebar.

The RSL was specifically designed to retrofit only the plastic hinge length of the reinforced concrete columns. This length, when subjected to cyclic loading, was estimated using the formula proposed by Paulay and Priestley [22] as in Equation (1).

$$\updownarrow_p = 0.08\updownarrow + 0.022 d_b f_y \tag{1}$$

Here, $\updownarrow_p$ is the plastic hinge length, $\updownarrow$ is the height of the column, d_b is the diameter of the longitudinal bar, and f_y is the yield strength of the longitudinal reinforcement.

In previous research [18] involving cyclic loading tests, the plastic hinge lengths predicted by Equation (1) were similar to the experimentally observed plastic hinge regions in reinforced concrete columns. This confirmation led to the use of the equation to calculate the plastic hinge length in the present study, which was 338 mm. To facilitate fabrication and construction, the section 375 mm from the base of the column was identified as the anticipated plastic hinge region and retrofitted with the RSL. The components of the RSL method, the steel link and steel plate, were made using steel with a yield strength of 275 MPa. The steel link was designed as a lightweight square hollow section to simplify replacement, with dimensions of 20 mm in width and 1.5 mm in thickness. The length of the steel link was based on the RSL retrofitting length, which matched the plastic hinge length of the reinforced concrete column. To enable installation of the steel link at a 45-degree angle within the plastic hinge region, its length was 455 mm. The steel plate used to connect the structural members was 200 mm wide, 250 mm deep, and 10 mm thick, with an 8-mm-thick hinge welded to the bottom plate. The steel link was secured to the bottom plate's sliding slot using 10-mm-diameter high-tensile strength bolts. The steel plate was attached to both the column and the foundation with 16-mm-diameter chemical anchors. The details of the test specimen are shown in Figure 6.

The RSL system was retrofitted to the reinforced concrete columns using the process shown in Figure 7. The replacement of a damaged RSL system after an earthquake is carried out in the reverse order of this construction process. If the structural members are not significantly damaged, it may be sufficient to replace only the steel link without needing to replace the steel plate.

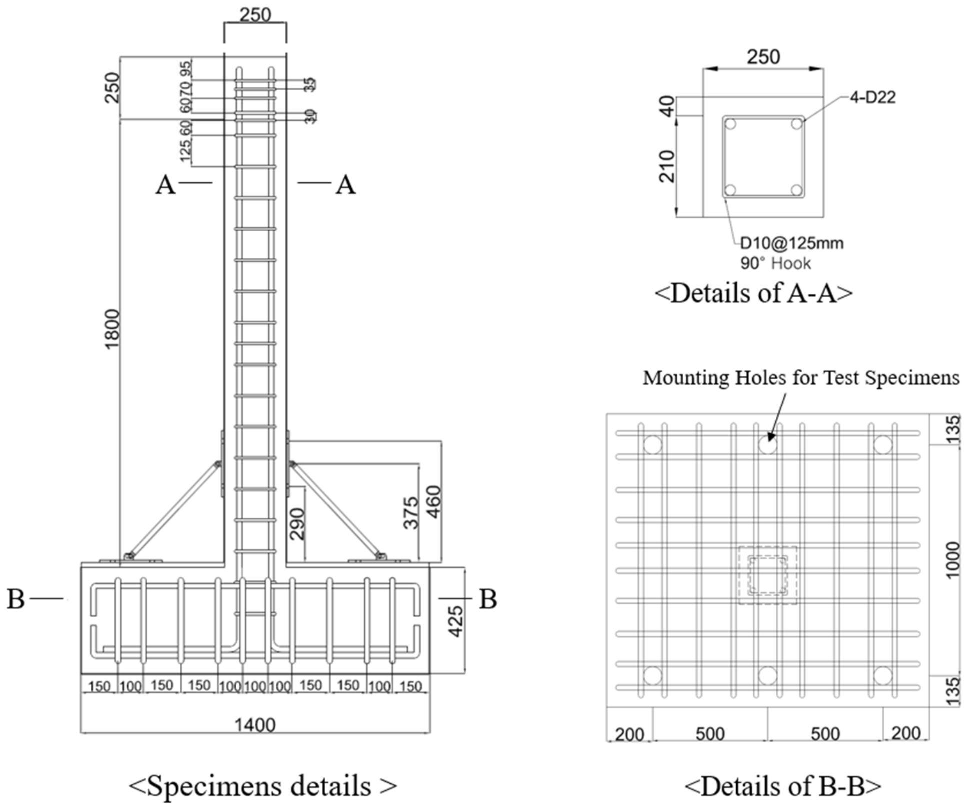

(**a**)

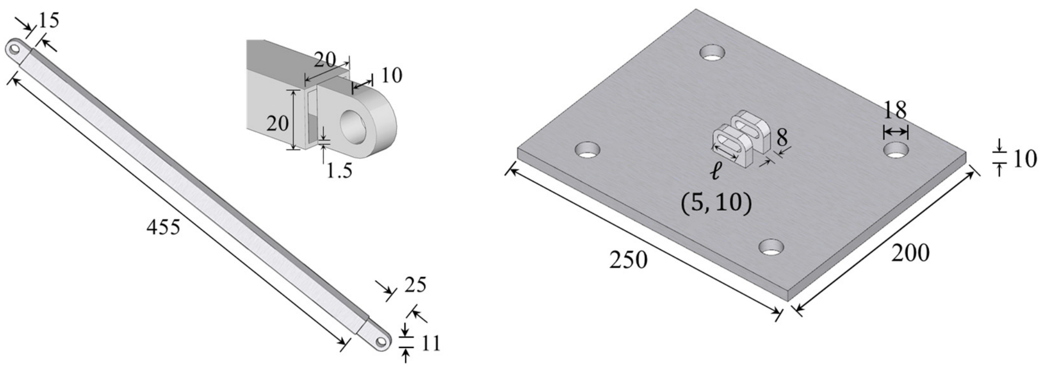

(**b**)

Figure 6. Details of the specimen [mm]: (**a**) RC column and (**b**) RSL system.

(**a**) (**b**) (**c**) (**d**)

Figure 7. Construction process: (**a**) surface treatment, (**b**) drilling, (**c**) joining the steel plate to the structural element with chemical anchors, and (**d**) connecting the steel link to the steel plate.

(1) Surface treatment of the retrofitting location for the RSL system.
(2) Drilling into the reinforced concrete column and beam.
(3) Joining the steel plate to the reinforced concrete column and beam using chemical anchors.
(4) Securing the steel link to the steel plate with high-tensile strength bolts.

3.2. Test Setup

In this research, cyclic loading involving eccentric lateral forces was applied to simulate the torsional effects of seismic loads on structures. A specialized jig was used to apply axial and lateral forces at specific points on the test specimens, and the experimental setup is illustrated in Figure 8. For clarity, the front of the specimen was designated as Side 1, while the other sides were labeled Sides 2, 3, and 4 in a clockwise direction. Lateral forces were introduced using a hydraulic actuator with a capacity of up to 1000 kN, controlled through displacement. The hydraulic actuator was positioned between the reaction wall and the specimen, connected to the top of the column through a jig. This jig, situated at both ends of the column's top and linked with steel rods, ensured a uniform introduction of loads in two directions during cyclic loading. The experiment involved varying the eccentricity of the applied lateral force, including scenarios with no eccentricity and eccentricities of 65 mm and 130 mm. This variation aimed to scrutinize the dynamic behavior of RSL-retrofitted reinforced concrete columns. The loading protocol adhered to the guidelines of ACI 374 [23], which defines the standards for structural experiments on moment-frame structures. The following loading protocol was adopted for assessing structural performance through cyclic loading:

(1) The initial drift ratio should fall within the range of linear elastic behavior.
(2) Subsequent drift ratios should not exceed 0.25% and then should not surpass 0.5%.
(3) The steps between subsequent drift ratios should be judiciously chosen, ensuring the experiment progresses up to a drift ratio of 3.5%.
(4) Each drift ratio should be repeated for three cycles of cyclic loading.

Accordingly, in this study, cyclic load testing was conducted for each drift ratio over three cycles. The initial drift ratio was set to 0.2%, with a subsequent ratio of 0.25%, and the experiment was planned to conclude when the load on the specimen was reduced to less than 80% of the maximum load after reaching the peak. The drift ratio is defined as the lateral displacement of a column at the point of load application (1800 mm from the bottom) divided by the column's height. To simulate real seismic loads acting on columns, constant axial forces were applied using a hydraulic jack. Columns with an axial load ratio exceeding 0.3 are less likely to exhibit nonlinear behavior and are more prone to brittle failure, while those with a ratio greater than 0.6 have almost no ductility due to excessive axial load [24,25]. Therefore, an axial load ratio of 0.17 was set to observe the dynamic behavior of the specimens. The axial load ratio was calculated as shown in Equation (2). For the test of the specimens in this study, a constant axial load of 255 kN, corresponding to an axial load ratio of 0.17, was applied to the top of the columns using a hydraulic jack.

$$\nu = \mathrm{P}/\mathrm{A_g f'_c} \tag{2}$$

Here, ν is the axial load ratio, P is the axial force introduced into the reinforced concrete columns, and A_g refers to the cross-sectional dimensions of the reinforced concrete columns.

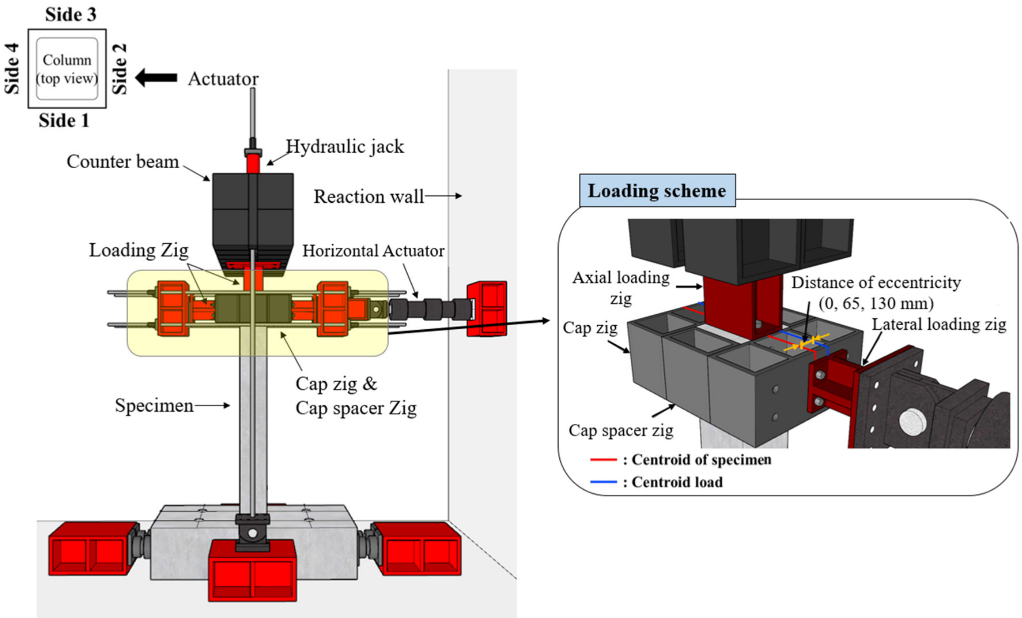

(**a**)

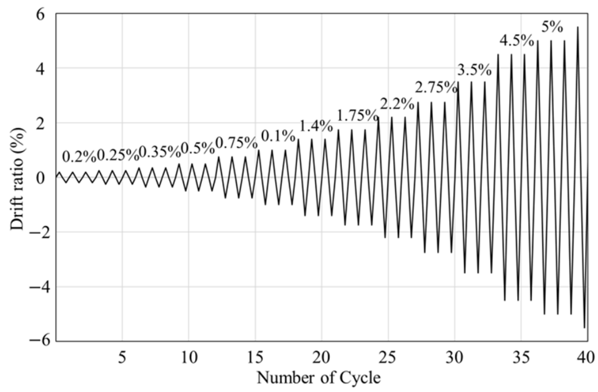

(**b**)

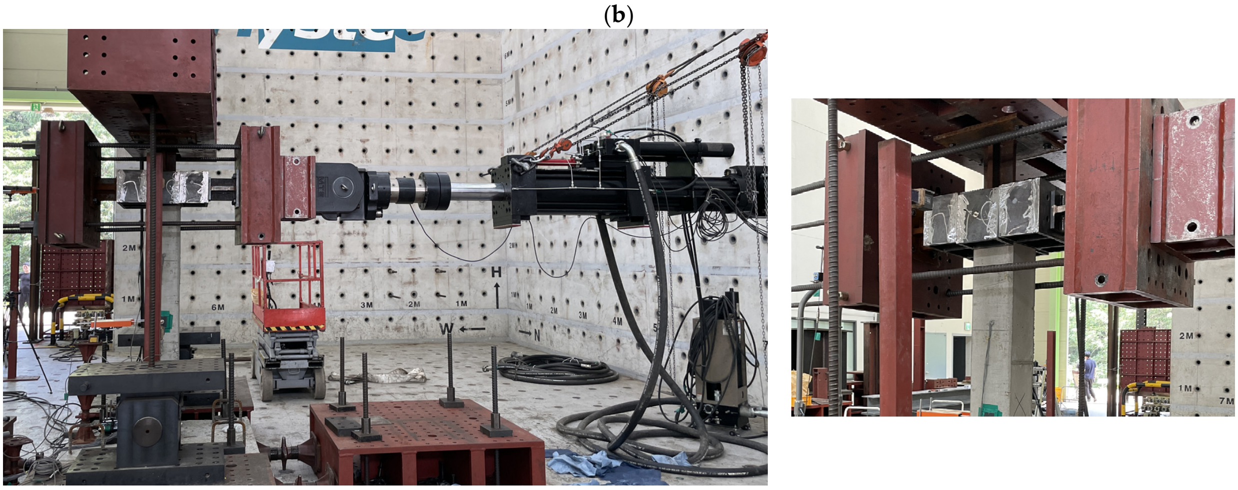

(**c**)

Figure 8. Test setup: (**a**) concept of the experiment, (**b**) loading protocol, and (**c**) photograph of the test setup.

4. Experimental Results and Analysis

4.1. Crack Propagation and Failure Modes

Figure 9 illustrates the propagation of cracks in each test specimen on side 2. Flexural cracks at the bottom of the column emerged in all specimens when the drift ratio reached

0.75%. As the load intensified, shear cracks developed and extended, eventually leading to concrete spalling at the bottom of the column. The experimental plan aimed to conclude the tests when the load dropped to 80% or less of the maximum after reaching the peak load, a point reached by all specimens at a drift ratio of 4.5%. The key initiation points for primary cracks in each specimen are summarized in Table 2. When comparing crack patterns among specimens with different eccentric distances, specimens NE-5 and E65-5, both featuring a sliding slot length of 5 mm and eccentric distances of 0 mm and 65 mm, respectively, exhibited similar patterns. In both cases, flexural cracks were distributed evenly throughout the column with an increasing drift ratio. Shear cracks manifested at a drift ratio of 2.2%, leading to concrete spalling in the first cycle at a drift ratio of 4.5%, concluding the experiment. Specimen E130-5, with a sliding slot length of 5 mm and an eccentricity of 130 mm, showed shear cracks at a lower drift ratio of 1.75%. These cracks concentrated at the bottom of the column, resulting in concrete spalling at a drift ratio of 3.5%, prompting the conclusion of the experiment at 4.5%. Specimen NE-10, featuring a sliding slot length of 10 mm and no eccentricity, exhibited shear cracks at a drift ratio of 2.2%, with concrete spalling observed at the column's bottom at a drift ratio of 4.5%. Similarly, in specimens with a 10 mm sliding slot length and an increased eccentricity of 130 mm, there was an acceleration in crack propagation. In these cases, shear cracks emerged at a drift ratio of 1%, with concrete spalling observed at a drift ratio of 3.5%.

The point at which the steel links began to resist load was visually inspected, as shown in Figure 10. Regardless of eccentricity, the steel links in specimens with a 5 mm sliding slot length commenced load resistance at a drift ratio of 1% and experienced buckling at 2.2%. Similarly, for specimens with a 10 mm sliding slot length, the steel links began resisting the load at a drift ratio of 1.4% and buckled at 2.75%, showing a consistent response across eccentricities. The point at which the steel links started resisting loads influenced the number and width of shear cracks in the reinforced concrete columns. The difference in the load-resisting initiation points resulted in fewer shear cracks in specimens with a 5 mm sliding slot length compared to those with a 10 mm length.

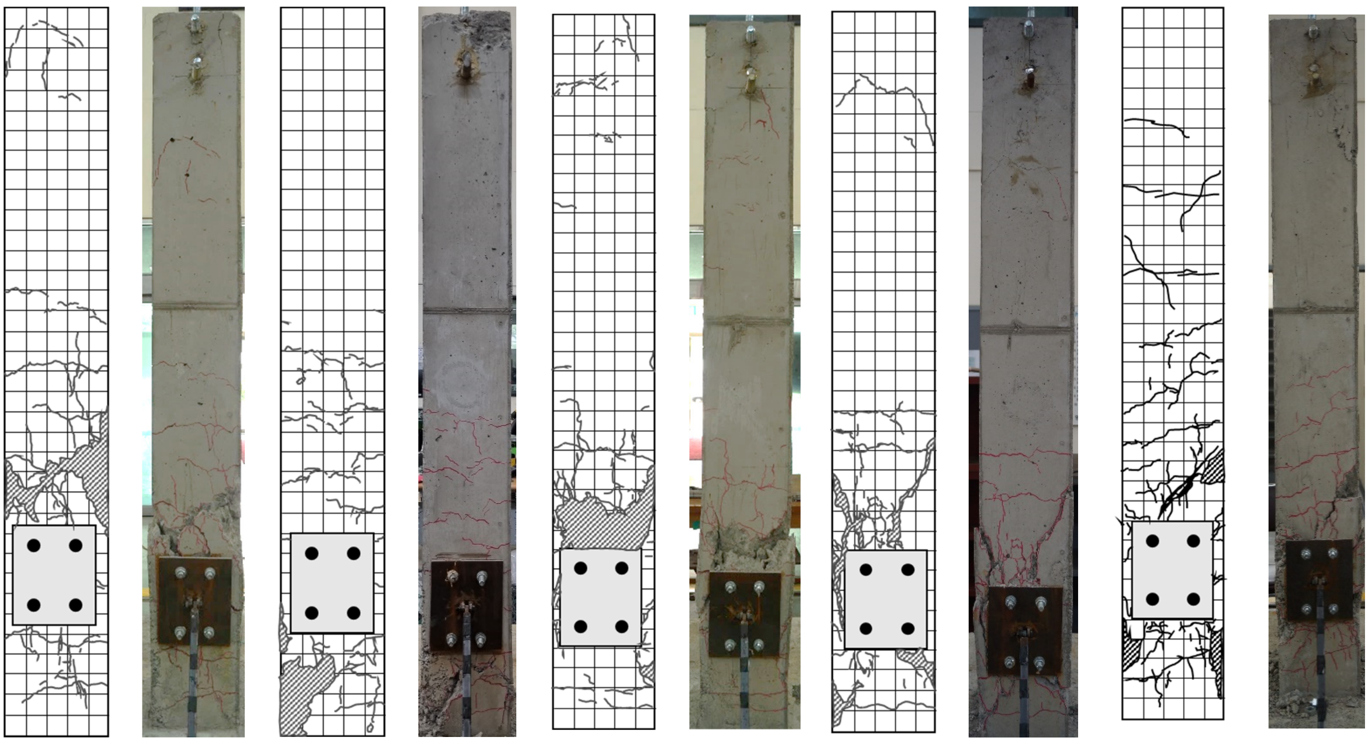

(**a**) (**b**) (**c**) (**d**) (**e**)

Figure 9. Crack propagation: (**a**) NE-10, (**b**) E130-10, (**c**) NE-5, (**d**) E65-5, and (**e**) E130-5.

Table 2. Initiation of crack occurrence.

Specimen	Drift Ratio (%)				
	Initial Crack	Shear Crack	Steel Link Buckled	Concrete Spalling	Terminate Experiment
NE-10	0.75	2.2	2.75	4.5	4.5
E130-10	0.75	1	2.75	3.5	4.5
NE-5	0.75	2.2	2.2	4.5	4.5
E65-5	0.75	2.2	2.2	4.5	4.5
E130-5	0.75	1.75	2.2	3.5	4.5

(**a**) (**b**)

Figure 10. (**a**) A steel link that came into contact with the end of the sliding slot and (**b**) the buckling of the steel link.

Cracks significantly impacting the failure of the test specimens were shear cracks originating at the bottom of the columns. Therefore, Table 3 presents the crack patterns observed at the bottom of the columns from side 1 at the point of failure. While the initiation of flexural cracks was identical for all specimens, the onset of shear cracks varied with the length of the sliding slot and eccentric distance. An increase in eccentric distance and a sliding slot length of 10 mm, as opposed to 5 mm, led to the earlier development of shear cracks. The effect of eccentric distance on the timing of shear crack initiation is attributed to the increased torsion on the specimen as the eccentric distance increases, resulting in an increase in the number and width of cracks and a rapid propagation of existing flexural cracks into shear cracks. The effect of sliding slot length on the crack propagation pattern, considered at the design stage, was validated through the experimental results, affirming the conceptual validity of the RSL system's retrofitting strategy.

As seen in Figure 11, no loosening of bolts or deformation of steel plates in the RSL system was observed at the termination of the experiment, suggesting that the system functioned effectively throughout the experiment. Since no deformation occurred in the steel plates after the experiment, the buckled and damaged steel links could be replaced simply by releasing the high-tensile bolts attached to the slot, affirming the RSL system's effectiveness as a structural fuse.

Table 3. Crack propagation.

Variables	Crack Propagation at the Bottom of the Column		Observed Damage
	E130-10	E130-5	
Sliding slot length			- Severe spalling of the concrete - As the length of the sliding slot increases, the number of flexural and shear cracks increases
	NE-5	E65-5	
Eccentric distance			- As the eccentric distance increases, the number of flexural cracks decreases, while the incidence of shear cracks becomes more frequent, and the width of these shear cracks increases significantly

(**a**) (**b**) (**c**)

Figure 11. RSL system after testing: (**a**) steel plate, (**b**) bolt, and (**c**) after removing the buckled steel link.

4.2. Load-Displaement Relationship

Figure 12 presents the load–displacement curves for each test specimen retrofitted with the RSL system. All specimens reached their maximum load at a drift ratio of 2.75%, followed by a decrease in load to less than 80% of the maximum at a drift ratio of 4.5%

due to shear cracks and concrete spalling at the bottom of the column. The maximum load increased as the sliding slot length and eccentric distance decreased. For specimens with a 5 mm sliding slot length, NE-5, E65-5, and E130-5, the maximum loads were 76.8 kN, 62.0 kN, and 55 kN, respectively, while those with a 10 mm sliding slot length, NE-10 and E130-10, had maximum loads of 73.9 kN and 52.4 kN. The maximum load decreased in all specimens as the eccentric distance increased, and the torsion also increased. Regardless of the sliding slot length, the maximum load for specimens with an eccentricity of 130 mm was about 70% of that for specimens without eccentricity. The maximum load for E65-5, with an eccentric distance of 65 mm and a 5 mm sliding slot, was about 81% of that for NE-5, which had no eccentricity. Previous research [26] showed a maximum load of about 60% in reinforced concrete columns subjected to eccentric lateral forces compared to columns without eccentricity. Therefore, it is evident that the RSL system effectively resists torsion. Even with a doubling of the eccentric distance, the reduction in maximum load was only about 10%, indicating that brittle failure was not observed despite increased torsion. Regardless of the eccentric distance, the difference in maximum load due to the length of the sliding slot was about 5%. While there was a tendency for the maximum load to decrease with increasing sliding slot length, the difference was minimal. This phenomenon likely occurred because the experiment was terminated after both the column and steel link fully resisted the load. This suggests that the length of the sliding slot had a minimal impact on the maximum load capacity.

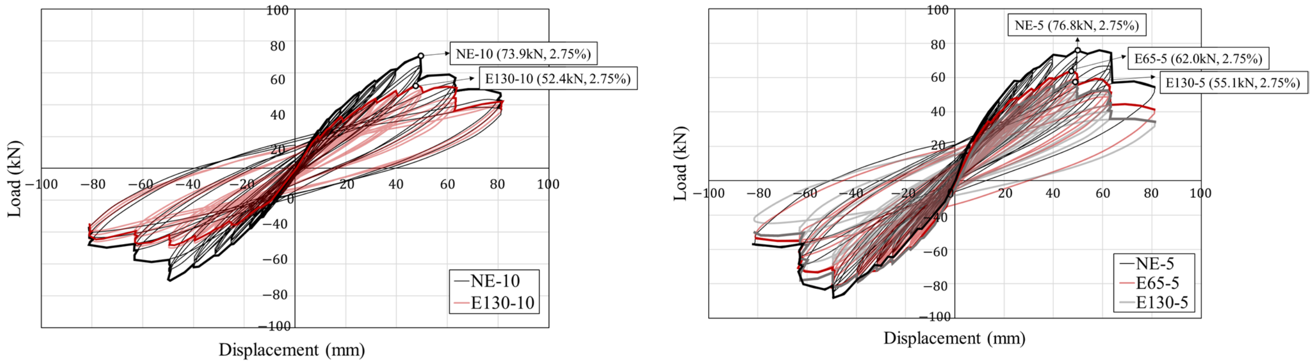

(**a**) (**b**)

Figure 12. Load–displacement curves: (**a**) 10 mm sliding slot length and (**b**) 5 mm sliding slot length.

4.3. Torsional Moment versus Twist Response

In this study, cyclic load testing with eccentric lateral forces was conducted to consider the effects of torsion on reinforced concrete columns during actual earthquakes. Based on the experimental results, the torsional moment and twist angles were calculated, and the relationship between them was used to analyze the seismic performance of the RSL system. The twist and torsional moment were determined using Equations (3) and (4), respectively. Specifically, to calculate the twist, Linear Variable Differential Transformers (LVDTs) were installed at the top of the columns, as shown in Figure 13, and the twist was determined by the difference in displacement measured by the LVDTs.

$$\mathrm{M_i} = \mathrm{P} \times \ell \times \cos\theta_\mathrm{i} \tag{3}$$

$$\theta_\mathrm{i} = \tan^{-1}\left(\frac{\Delta_2 - \Delta_1}{\mathrm{d}}\right) \tag{4}$$

Here, M_i is the torsional moment generated in the specimen at the i-th drift ratio, P is the maximum load at the i-th drift ratio, ℓ is the eccentric distance, θ_i is the twist of the column cross section, d represents the distance between the LVDTs, and $\Delta_{1,2}$ denotes the displacement value measured by the LVDTs.

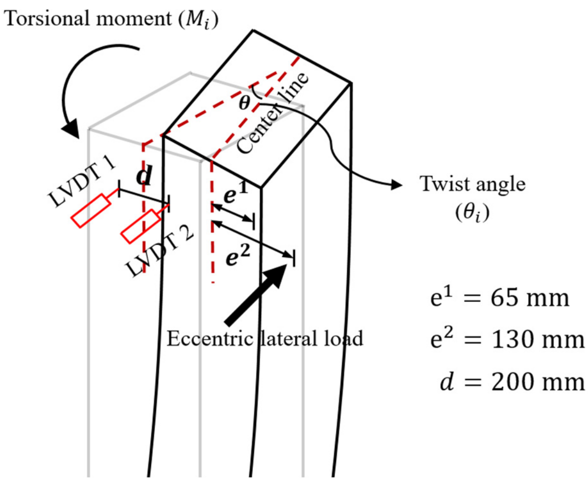

Figure 13. Measurement methods for torsional moment and twist angle of columns.

Figure 14 shows the torsional moment–twist envelopes for each specimen. As NE-5 and NE-10 had no eccentric distance and, thus, no torsion, the torsional moments and twist angles for specimens E65-5, E130-5, and E130-10, which were subjected to eccentric lateral loads, were analyzed. The torsional moments and twist angles at key points for these specimens are summarized in Table 4. For all specimens, the twist angles and torsional moments were calculated from the first cycle at each drift ratio.

Table 4. Comparison of the torsional performance of specimens subjected to eccentric lateral loads.

Point	Results	E130-10		E65-5		E130-5	
		(+)	(−)	(+)	(−)	(+)	(−)
Initial crack	M_T (kN·m)	3.03	3.04	2.19	2.01	3.70	3.20
	θ_T (degree)	0.35	−0.40	0.15	−0.24	0.30	−0.36
Shear crack	M_T (kN·m)	3.81	3.37	3.61	3.57	5.57	5.14
	θ_T (degree)	0.50	−0.46	0.37	−0.31	0.38	−0.39
Maximum	M_T (kN·m)	5.66	5.46	3.70	3.76	6.19	5.99
	θ_T (degree)	0.62	−0.56	0.41	−0.34	0.51	−0.47
Termination	M_T (kN·m)	4.73	4.00	2.83	3.25	4.82	4.78
	θ_T (degree)	0.68	−0.84	0.51	−0.43	0.60	−0.54

M_T: Torsional moment, θ_T: Twist angle.

At all drift ratios, the torsional moments and twist angles for E130-5 and E130-10, which had a larger eccentric distance, were significantly higher than those for E65-5. This is attributed to the greater torsion induced in the specimens as the eccentric distance increases. Comparing the torsional moments and twist angles of E65-5 and E130-5 at the point of major crack initiation, the torsional moment and twist angle for E130-5 were approximately 1.7 and 2 times higher than those for E65-5 at the initial crack, 1.5 and 1.1 times higher at the shear crack, and 1.7 and 1.2 times higher at the maximum values, respectively. After the initial crack, both specimens showed reduced stiffness due to crack initiation, leading to a slight decrease in the difference attributed to the eccentric distance. Subsequent reduction occurred in the increase of twist angle with load increase as the RSL system began to resist torsion. The reductions in torsional moment from maximum to the end of the experiment for E65-5 and E130-5 were 80% and 70%, respectively, indicating more frequent brittle failure due to increased torsion with larger eccentric distances.

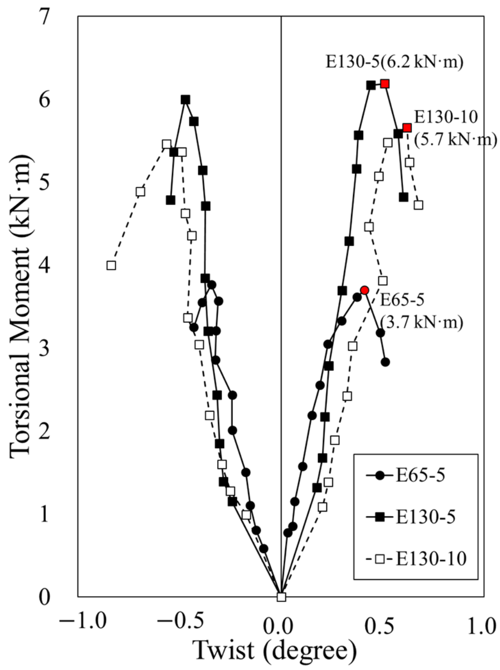

Figure 14. Torsional moment–twist envelopes.

In comparison of torsional moments and twist angles for specimens E130-5 and E130-10 at the same drift ratios, E130-10 exhibited larger twist angles, suggesting a greater torsional load in this specimen. In particular, at the point of flexural crack initiation, the twist angle for E130-5 was 85% of that for E130-10, indicating greater torsion in E130-10, where the steel link did not yet resist the load. After the steel link in E130-5 started resisting the load, the increase in twist angle was restrained. At the maximum point, the twist angle was approximately 34% higher than at the initiation of the shear crack. In E130-10, the twist angle increased by 43% before shear crack initiation and by 24% from shear crack to the maximum value, showing a minimal increase. These findings suggest that the steel link effectively resisted the load and reduced torsion in the reinforced concrete column. The minimal difference in torsional moment and twist angle at the end of the experiment compared to the values just before the final drift ratio in specimens E65-5, E130-5, and E130-10 suggests that retrofitting reinforced concrete columns with the RSL system could prevent brittle failure due to torsion.

4.4. Strain

The main distinction between the RSL retrofitting method and conventional bracing techniques lies in the movement of the steel link, attached to the bottom plate with high-tensile bolts within a sliding slot, laterally in response to lateral displacements acting on the column. Within the permissible displacement of the sliding bolt, the steel link behaves elastically. When this permissible displacement is exceeded and an excessive load is applied, the steel link is buckled. Consequently, the behavior of the RSL method varies with the sliding slot length, which can be adjusted to enable the RSL to function effectively as a structural fuse.

In this study, the behavior of the steel link was analyzed experimentally by observing the strain distribution at different drift ratios using gauges attached to the steel link. The gauges were aligned along the length of the steel link, but the analysis focused on the gauge positioned in the middle, where the highest strain was recorded. This analysis is depicted in Figure 15. The yield strength of the steel link was 275 MPa, and its yield strain was 1375 $\mu\varepsilon$. The deformation behavior of the steel link demonstrated a pattern across various eccentric distances and sliding slot lengths. The steel link underwent lateral movement within the sliding slot, initiating load resistance once the displacement exceeded the sliding slot length, eventually reaching the slot end. In specimens with a 5 mm sliding slot, load resistance was anticipated to begin at a drift ratio of 0.75%. The analysis showed that deformation in the steel link commenced at a 1% drift ratio and yielded at 2.2%. For specimens with a 10 mm sliding slot, resistance to load started at a drift ratio of 1.4%, with deformation occurring at this point and yielding observed at 2.75%. Specimens with a 5 mm slot yielded earlier and exhibited a higher final strain compared to those with a 10 mm slot. The strain in the steel link increased with the eccentric distance, a phenomenon attributed to the increased torsion exerted on the specimens.

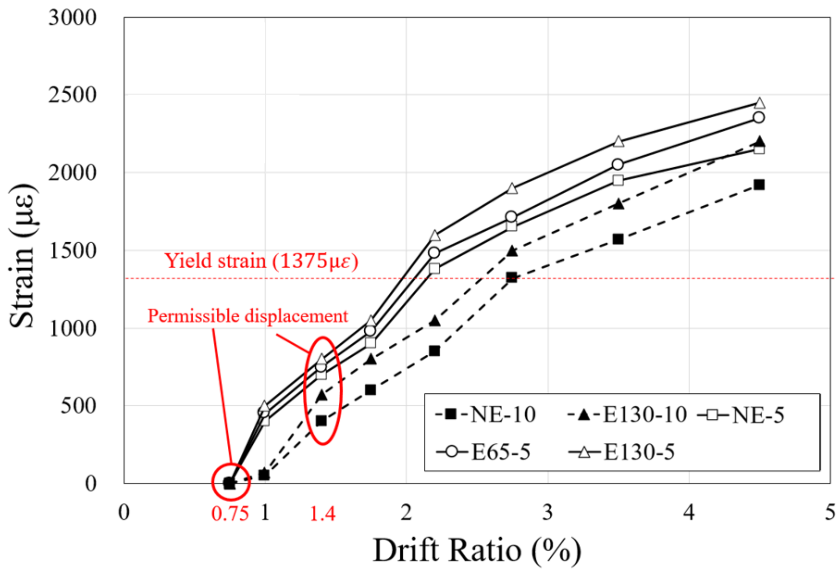

Figure 15. Strain of the steel link.

The visual inspection of the steel link revealed a buckling point at a drift ratio of 2.2% for the 5 mm slot and 2.75% for the 10 mm slot, accompanied by a noticeable increase in strain observed before these points. Given the tendency of reinforced concrete columns to exhibit brittle behavior after the longitudinal reinforcement yields, with rapid crack propagation in the concrete, it becomes crucial to identify the yield point of the longitudinal reinforcement. Figure 16 illustrates the strain distribution along the height of the longitudinal reinforcement from the base of the column. Across all specimens, the strain in the longitudinal reinforcement increased from the middle to the bottom of the column, reaching its peak at the bottom. The yield strain for the longitudinal reinforcement of deformed bars with a yield strength of 400 MPa corresponds to 2000 με.

The RSL method is specifically designed to retrofit the expected plastic hinge regions of reinforced concrete columns. Normally, the strain in the longitudinal reinforcement of columns sharply increases at the bottom. However, in RSL-retrofitted specimens, cracking and deformation were dispersed toward the middle of the column, resulting in an even distribution of strain along the column height. In specimens with a 5 mm sliding slot, the longitudinal reinforcement in specimens with eccentric distances of 0 and 65 mm yielded at drift ratios of 2.75% and 2.2%, respectively, with an eccentric distance of 130 mm. For the 10 mm slot, specimens with eccentric distances of 0 and 130 mm yielded at drift ratios of 3.5% and 2.75%, respectively. All specimens exhibited an increase in strain in the upper part of the column with increasing eccentric distance, likely attributed to increased torsion.

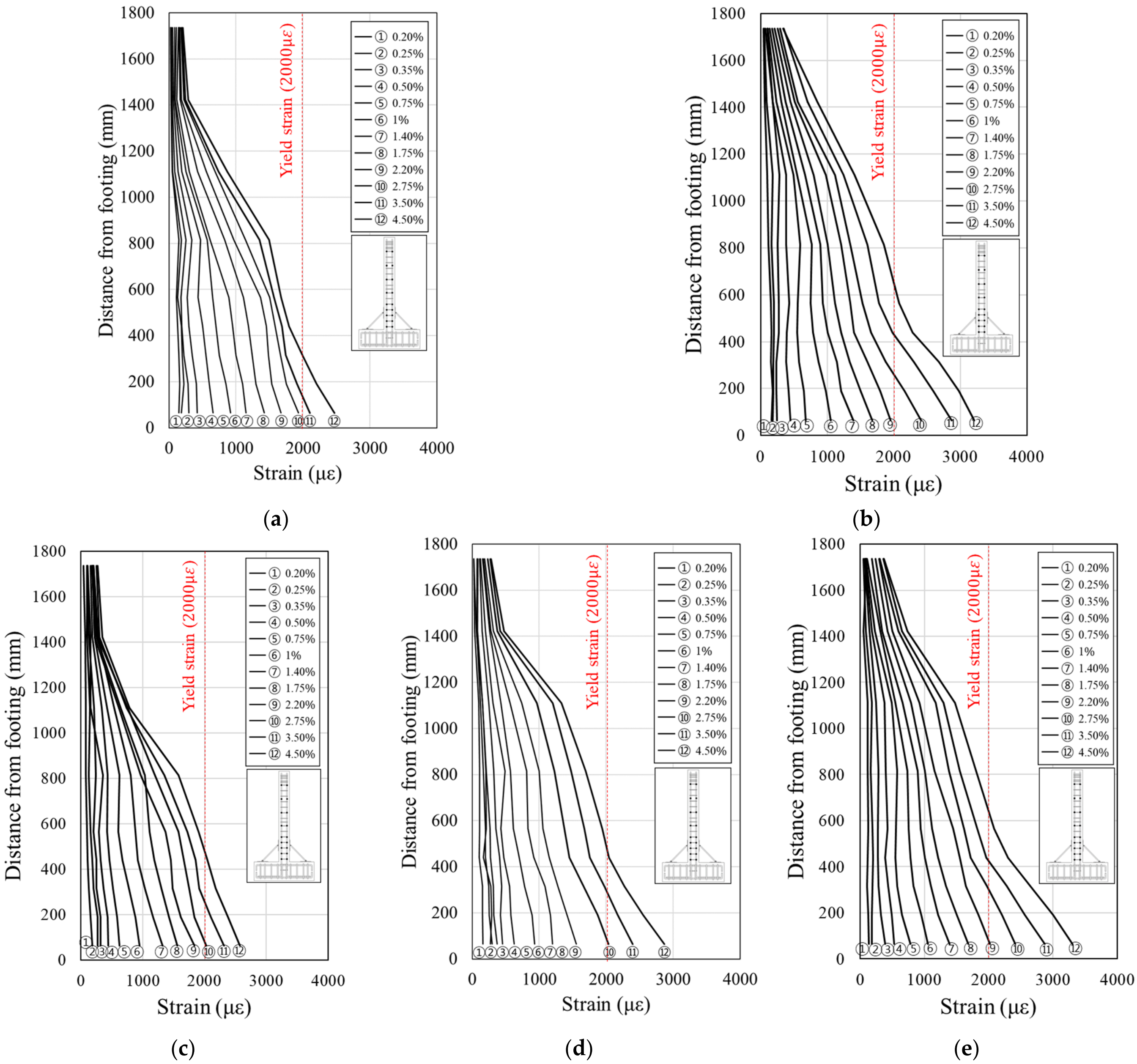

Figure 16. Strain of longitudinal reinforcement. (**a**) NE-10, (**b**) E130-10, (**c**) NE-5, (**d**) E65-5, and (**e**) E130-5.

Specimens with a 10 mm sliding slot demonstrated delayed yielding of the longitudinal reinforcement compared to those with a 5 mm slot, correlated with the yielding point of the steel link. Following the yield of the steel link, the reinforced concrete column resists the lateral load, elevating the load on the longitudinal reinforcement. Initially, the load is borne by the reinforced concrete column. As the lateral displacement on the column exceeds the permissible displacement of the steel link, the link starts to bear the load. When the steel link undergoes excessive deformation and either buckles or yields, the reinforced concrete column once again assumes a significant portion of the load. Consequently, the RSL system functions as a sacrificial element, effectively preventing damage to the structural elements.

4.5. Energy Dissipation

The energy dissipation capacity, a critical factor in assessing seismic performance, refers to the ability of a structure to absorb seismic energy. The higher this capacity is, the more it can reduce damage caused by earthquakes. This capacity is calculated from the area under the load–displacement curve obtained from cyclic load tests. The cumulative energy dissipation for each specimen at different drift ratios is summarized in Table 5. Figure 17 illustrates the normalized cumulative energy dissipation capacity at the conclusion of the experiments, using the specimen exhibiting the highest cumulative energy dissipation as a benchmark. In Figure 17a, the data are normalized to those of the NE-10 specimen to investigate the effect of sliding slot length on the cumulative energy dissipation capacity. Conversely, Figure 17b employs NE-5 as the normalization reference to evaluate the influence of eccentric distance on the cumulative energy dissipation capacity.

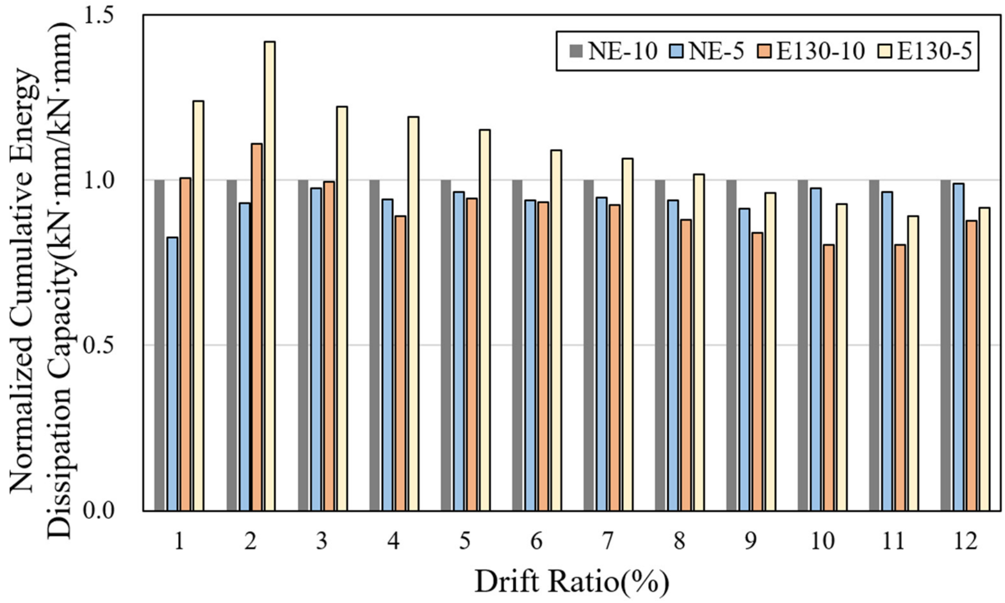

(**a**)

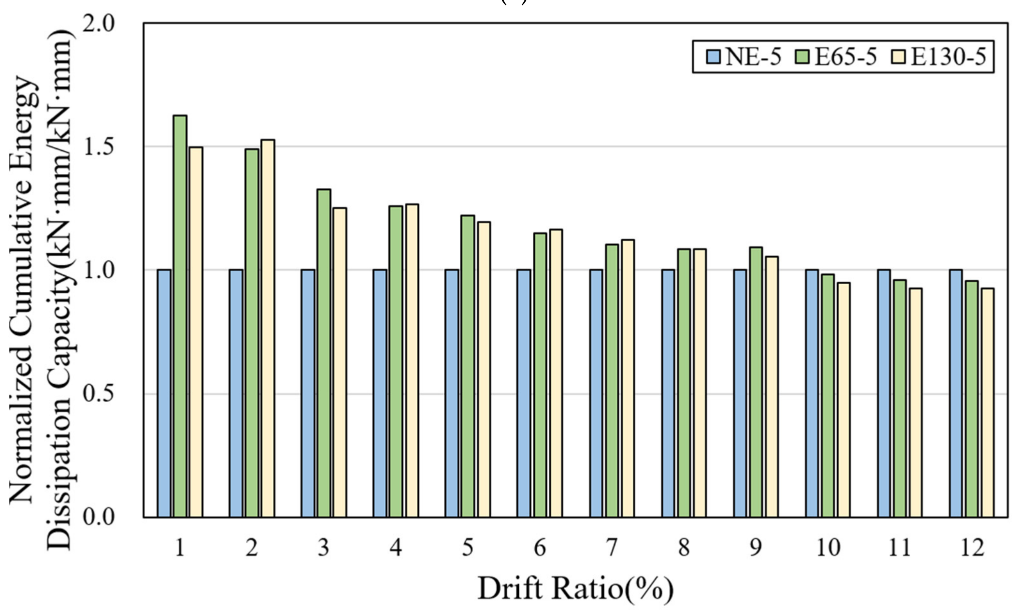

(**b**)

Figure 17. Normalized cumulative energy dissipation capacity: (**a**) effect of sliding slot length and (**b**) effect of eccentric distance.

Table 5. Cumulative energy dissipation capacity of the specimens.

Drift Ratio (%)	Cumulative Energy Dissipation Capacity (kN·mm)				
	NE-10	**E130-10**	**NE-5**	**E65-5**	**E130-5**
0.2	10.8	10.9	9.0	14.6	13.4
0.25	23.8	26.5	22.2	33.1	33.9
0.35	51.1	50.9	49.9	66.2	62.6
0.5	107.4	95.8	101.3	127.4	128.1
0.75	222.0	209.5	214.2	262.0	255.7
1	404.1	377.1	379.4	436.5	441.1
1.4	740.0	684.4	701.7	775.6	788.1
1.75	1180.1	1038.6	1109.0	1201.8	1201.7
2.2	1893.6	1591.7	1728.6	1885.7	1821.8
2.75	3153.3	2537.4	3078.5	3019.3	2924.8
3.5	5723.4	4611.2	5520.4	5306.6	5105.5
4.5	9236.1	8092.6	9143.1	8754.0	8456.6

For specimens featuring a 5 mm sliding slot length, the cumulative energy dissipations for NE-5, E65-5, and E130-5 were 9143.1 kN·mm, 8754.0 kN·mm, and 8456.6 kN·mm, respectively. In the case of a 10 mm sliding slot length, NE-10 and E130-10 exhibited cumulative energy dissipations of 9236.1 kN·mm and 8092.6 kN·mm, respectively. The difference in cumulative energy dissipation attributable to the sliding slot length was approximately 1% for specimens without eccentricity and around 4% for those with a 130 mm eccentricity. However, a notable reduction of 8% in energy dissipation was observed for the 5 mm sliding slot length with increasing eccentricity, and a 12% reduction was noted for the 10 mm sliding slot length. These findings suggest a discernible difference in performance against torsion based on the sliding slot length. The augmentation of eccentricity induces greater torsion on the column, resulting in numerous shear cracks, diminishing stiffness, and reducing energy dissipation. The point at which the steel link commences resistance against the load varies with the sliding slot length, and the degree of damage to the reinforced concrete column before the steel link starts resisting the load also differs. This discrepancy leads to a more substantial reduction in cumulative energy dissipation for specimens with a delayed onset of resistance. Consequently, it is advisable to select the appropriate sliding slot length in accordance with the design intent when employing the RSL system as a structural fuse.

5. Conclusions

This study focused on the dynamic behavior of the Replaceable Steel Link (RSL) system, intended to serve as a structural fuse. Cyclic loading tests were carried out on the RSL system at sliding slot lengths, a key variable affecting its performance. The experiments assessed the behavior of reinforced concrete columns retrofitted with RSLs under realistic seismic loads. Torsional effects, reflecting the eccentricity of lateral forces, were also taken into account. In essence, this study contributes to the understanding of the versatility and adaptability of the RSL system in seismic design, specifically in its role as a replaceable structural fuse under torsional load. It builds upon and extends the findings of previous research. The primary conclusions drawn from the study are as follows:

(1) The RSL system exhibited significant control over crack propagation in reinforced concrete columns. Initial flexural cracks were observed at a drift ratio of 0.75% in all specimens. Under eccentric loading, specimens with a 5 mm sliding slot length showed shear cracks at a drift ratio of 1.75%. In comparison, specimens with a 10 mm sliding slot length exhibited shear cracks at a drift ratio of 1%. These findings

indicate that the sliding slot length plays a crucial role in crack propagation. After the experiment concluded, the damaged steel link could be easily replaced, thus confirming the feasibility of using the RSL system as a structural fuse.

(2) The maximum load capacities exhibited variations based on sliding slot length and eccentric distance. An increase in eccentric distance resulted in a 70 to 80% change in maximum load capacity, while the variation in maximum load due to sliding slot length at the same drift ratio was around 10%. This finding underscores the RSL system's capability to effectively resist torsion. Specimens with a 5 mm slot reached their yield strain earlier and showed a higher strain compared to those with a 10 mm slot. This result was in line with the initial design expectations, demonstrating that adjustment of the sliding slot length can be an effective method to regulate the yielding behavior of a steel link.

(3) The study analyzed torsional moments and twist angles at various drift ratios, notably at the onset of major cracks. In all specimens, there was only a minimal difference in torsional moment and twist angle at the conclusion of the experiment compared to the measurements just before reaching the final drift ratio. This outcome suggests that retrofitting reinforced concrete columns with the RSL system can effectively prevent brittle failure due to torsion.

(4) The difference in cumulative energy dissipation due to variations in sliding slot length was marginal, ranging from 1 to 4%. However, with an increase in sliding slot length, the difference in cumulative energy dissipation attributable to augmented eccentric distances reached approximately 50%. This indicates a notable impact of sliding slot length on the system's ability to resist torsion. Consequently, it is recommended that the length of the sliding slot be based on the specific seismic design objectives when employing the RSL system as a structural fuse.

(5) This study investigated the behavior of reinforced concrete columns retrofitted with the RSL system under torsional loads, highlighting the system's potential as a structural fuse. Despite this, the complexity inherent in analyzing structural fuse systems like the RSL is well recognized. Therefore, further research should be conducted to develop analysis methods for RSL systems. Such research should incorporate a range of variables, including sliding slot length, column dimensions, and material properties, to facilitate the effective application of RSLs as structural fuses.

Author Contributions: Conceptualization, K.M.R. and Y.H.L.; methodology, K.M.R. and M.S.K.; validation, Y.H.L.; formal analysis, K.M.R. and M.S.K.; investigation, K.M.R. and Y.H.L.; writing—original draft preparation, K.M.R.; writing—review and editing, Y.H.L. All authors have read and agreed to the published version of the manuscript.

Funding: This work was supported by a National Research Foundation of Korea (NRF) grant funded by the Korean government (MSIT) (No. 2019R1A2C1090033 and No. 2020R1A2C2009351).

Institutional Review Board Statement: Not applicable.

Informed Consent Statement: Not applicable.

Data Availability Statement: The data is contained within the article.

Conflicts of Interest: The authors declare no conflicts of interest.

References

1. Attari, N.; Youcef, Y.S.; Amziane, S. Seismic performance of reinforced concrete beam–column joint strengthening by frp sheets. *Structures* **2019**, *20*, 353–364. [CrossRef]
2. Li, Y.; Yin, S.; Chen, W. Seismic behavior of corrosion-damaged RC columns strengthened with TRC under a chloride environment. *Constr. Build. Mat.* **2019**, *201*, 736–745.
3. Nasab, M.S.E.; Javidan, M.M.; Chun, S.; Kim, J. Experimental study on seismic retrofit of a RC frame using viscoelastic dampers. *Structures* **2021**, *34*, 771–786. [CrossRef]
4. Cheng, S.G.; Zhu, Y.X.; Zhang, W.P.; Shi, T.H. Study on the seismic performance of retrofitted RC frames with RC infill wall mega braces. *Eng. Struct.* **2021**, *233*, 111911. [CrossRef]

5. Ferraioli, M.; Lavino, A.; De Matteis, G. A design method for seismic retrofit of reinforced concrete frame buildings using aluminum shear panels. *Arch. Civ. Mech. Eng.* **2023**, *23*, 106. [CrossRef]
6. Vargas, R.; Bruneau, M. Analytical response and design of buildings with metallic structural fuses. *J. Struct. Eng.* **2009**, *135*, 386–393. [CrossRef]
7. El-Bahey, S.; Bruneau, M. Structural fuse concept for bridges. *Transp. Res. Rec.* **2010**, *2202*, 167–172. [CrossRef]
8. Nikoukalam, M.T.; Dolatshahi, K.M. Development of structural shear fuse in moment resisting frames. *J. Constr. Steel Res.* **2015**, *114*, 349–361. [CrossRef]
9. Irvani, M.; Ezati, H.; Khafajeh, R.; Jaari, V.R.K. Numerically study on the seismic response of partially restrained moment connection with structural fuse T-stub for European sections. *Structures* **2022**, *35*, 82–105. [CrossRef]
10. Farzampour, A. Innovative structural fuse systems for various prototype applications. *Materials* **2022**, *15*, 805. [CrossRef]
11. Ghadami, A.; Pourmoosavi, G.; Ghamari, A. Seismic design of elements outside of the short low-yield-point steel shear links. *J. Constr. Steel Res.* **2021**, *178*, 106489. [CrossRef]
12. Zhuang, L.; Wang, J.; Nie, X.; Wu, Z. Experimental study on seismic behaviour of eccentrically braced composite frame with vertical LYP steel shear link. *Eng. Struct.* **2022**, *255*, 113957. [CrossRef]
13. Qu, B.; Liu, X.; Hou, H.; Qiu, C.; Hu, D. Testing of buckling-restrained braces with replaceable steel angle fuses. *J. Struct. Eng.* **2018**, *144*, 04018001. [CrossRef]
14. Saravanan, M.; Goswami, R.; Palani, G.S. Replaceable fuses in earthquake resistant steel structures: A review. *Int. J. Steel Struct.* **2018**, *18*, 868–879. [CrossRef]
15. Al-Sadoon, Z.A.; Karzad, A.S.; Sagheer, A.; AlHamaydeh, M. Replaceable fuse buckling-restrained brace (BRB): Experimental cyclic qualification testing and NLFEA modeling. *Structures* **2022**, *39*, 997–1015. [CrossRef]
16. Pratap, M.; Vesmawala, G.R. The State-of-the-art review on development of replaceable fuse components in resilient moment resisting frame. *Structures* **2023**, *56*, 104888. [CrossRef]
17. Ullah, R.; Vafaei, M.; Alih, S.C.; Waheed, A. A replaceable sandwiched metallic fuse damper for seismic protection of braced frames. *Eng. Struct.* **2024**, *298*, 117072. [CrossRef]
18. Kim, M.S.; Lee, Y.H. Seismic Behavior of Concrete Columns Retrofitted with a Brace-Type Replaceable Steel Link. *Materials* **2023**, *16*, 1182. [CrossRef]
19. Xu, C.; Jin, L.; Ding, Z.; Li, D.; Du, X. Size effect tests of high-strength RC columns under eccentric loading. *Eng. Struct.* **2016**, *126*, 78–91. [CrossRef]
20. Huang, H.; Huang, M.; Zhang, W.; Pospisil, S.; Wu, T. Experimental investigation on rehabilitation of corroded RC columns with BSP and HPFL under combined loadings. *J. Struct. Eng.* **2020**, *146*, 04020157. [CrossRef]
21. *ACI 318-19*; Building Code Requirements for Reinforced Concrete and Commentary. American Concrete Institute: Farmington Hills, MI, USA, 2019.
22. Paulay, T.; Priestley, M.J.N. *Seismic Design of Reinforced Concrete and Masonry Buildings*; John Wiley & Sons, Inc.: Hoboken, NJ, USA, 1992.
23. *ACI 374.1-05*; Acceptance Criteria for Moment Frames Based on Structural Testing and Commentary. American Concrete Institute: Farmington Hills, MI, USA, 2005.
24. Al-Osta, M.A.; Khan, U.; Baluch, M.H.; Rahman, M.K. Effects of variation of axial load on seismic performance of shear deficient RC exterior BCJs. *Int. J. Concr. Struct. Mater.* **2018**, *12*, 46. [CrossRef]
25. Vu, N.S.; Li, B.; Tran, C.T.N. Seismic Behavior of Reinforced Concrete Short Columns Subjected to Varying Axial Load. *ACI Struct. J.* **2022**, *119*, 6.
26. Huang, H.; Hao, R.; Zhang, W.; Huang, M. Experimental study on seismic performance of square RC columns subjected to combined loadings. *Eng. Struct.* **2019**, *184*, 194–204. [CrossRef]